Available online at www.sciencedirect.com
ScienceDirect
Journal of Power Sources 173 (2007) 1024–1028
JOURNAL OF POWER SOURCES
www.elsevier.com/locate/jpowsour

Short communication

Carbon-supported, nano-structured, manganese oxide composite electrode for electrochemical supercapacitor

Raj Kishore Sharma, Hyung-Suk Oh, Yong-Gun Shul, Hansung Kim *

Department of Chemical Engineering, Yonsei University, 134 Shinchon-Dong, Seodaemun-gu, 120-749 Seoul, Republic of Korea

Received 11 May 2007; received in revised form 2 August 2007; accepted 8 August 2007
Available online 2 September 2007

Abstract

Carbon-supported MnO_2 nanorods are synthesized using a microemulsion process and a manganese oxide/carbon (MnO_2/C) composite is investigated for use in a supercapacitor. As shown by high-resolution transmission electron microscopy the 2 nm × 10 nm MnO_2 nanorods are uniformly dispersed on the carbon surface. Cyclic voltammograms recorded for the MnO_2/C composite electrode display ideal capacitive behaviour between −0.1 and 0.8 V (vs. saturated calomel electrode) with high reversibility. The specific capacitance of the MnO_2/C composite electrode found to be 165 F g^{-1} and is estimated to be as high as 458 F g^{-1} for the MnO_2. Based on cyclic voltammetric life-cycle tests, the MnO_2/C composite electrode gives a highly stable and reversible performance for up to 10,000 cycles.

Keywords: Supercapacitor; Manganese oxide; Composite electrode; Microemulsion; Specific capacitance

1. Introduction

In recent years, electrochemical supercapacitors have received a considerable amount of attention due to their ability to deliver high specific power [1]. Based on their fundamental charge-storage mechanism, supercapacitors are categorized as electrical double-layer capacitors (ELDCs) or Faradic pseudocapacitors. The former stores energy by charge separation at the electrode and electrolyte interface while the latter utilizes Faradic redox reactions.

Several transition metal oxides have been investigated as potential electrode materials for use in supercapacitors; their charge-storage mechanisms are based predominantly on pseudocapacitance [2,3]. Hydrous forms of ruthenium oxide have been found to possess very high capacitance due to redox transitions that go beyond the surface and penetrate into the bulk of the material [4,5]. Manganese oxides are seen to be potentially useful materials for pseudocapacitors not only due to their low cost but also to their environmental friendliness [6,7]. In the literature, the specific capacitance of manganese oxide is reported to be between 150 and 250 F g^{-1} at a loading level of 0.4–0.5 mg cm^{-2} [8]. Prasad and Miura [9,10] have reported a capacitance value between 400 and 621 F g^{-1} for amorphous electrolytic manganese dioxide (EMD) and MnO_2-based mixed oxides. Nevertheless, a higher capacitance (1370 F g^{-1}) is expected for MnO_2-based supercapacitor electrodes [2]. This performance can be achieved by enhancing the surface area and the material utilization. In order to enhance the material utilization direct deposition of manganese oxide on a carbon host, such as active carbon, carbon nanotubes, meso-porous carbon or large-area carbon, has been studied [11–13]. In addition to providing double-layer capacitance and creating a large surface area, the addition of carbon to a manganese oxide matrix improves conductivity by decreasing the ionic mass-transfer resistance. Consequently, an increase in both the specific power and energy of the electrode can be expected [14,15]. Among the various strategies used to increase the utilization of material via enhancing the surface area [16], the use of nano-structured MnO_2 as the electrode material is preferred [17].

One-dimensional (1D) nano-structures are the smallest structures that provide efficient electron transport. In this regard, efforts have been made to develop 1D MnO_2 nanorods and nanowires with various polymorphs [18–24]. Among the available techniques, the microemulsion process of nano-synthesis offers a precise control on particle size and shape; consequently, it has been utilized for nano-MnO_2 synthesis [25].

* Corresponding author. Tel.: +82 2 2123 5753; fax: +82 2 312 6401.
E-mail address: elchem@yonsei.ac.kr (H. Kim).

0378-7753/$ – see front matter © 2007 Elsevier B.V. All rights reserved.
doi:10.1016/j.jpowsour.2007.08.076

As a modification to this process, in the present study, a carbon material with a large surface area was added. This resulted in small nanorods with uniform dispersion. The addition of carbon increases the conductivity of materials and provides nucleation sites for the particles to grow. The high specific capacitance and long-term stability of the electrode suggest the use of the composite as a material for supercapacitor electrodes.

In the present study, the effect of adding a carbon support with a large surface area during the microemulsion synthesis of MnO_2 is investigated. The capacitance and long-term stability of the materials so produced are then examined.

2. Experimental

The following analytical grade reagents were obtained from Merck: $KMnO_4$, $Mn(CH_3COO)_2{\cdot}4H_2O$, sodium sulfo succinate as surfactant, isooctane, isopropyl alcohol, Nafion and Na_2SO_4. Large surface area ($248\,m^2\,g^{-1}$) carbon black (Vulcan XC-72, Cabot Corp., USA) was used as a support for the MnO_2 nanorods. Graphite plates were used to deposit the MnO_2/C composite.

2.1. Preparation of MnO_2/C composite material

Carbon-supported MnO_2 nanorods were prepared in a microemulsion medium. The microemulsion solution was prepared by mixing 15 g of the surfactant AOT in isooctane as the organic phase. The mixture was stirred vigorously for 2 h and then divided into three equal parts. A 40 mM aqueous solution of $KMnO_4$ was mixed with one part of the AOT solution and a 60 mM aqueous solution of $Mn(CH_3COO)_2{\cdot}4H_2O$ was mixed with the second part; 0.36 g of carbon black was dispersed in 20 ml of water by stirring and then mixed with the third part. Prior to mixing together, these three microemulsion solutions were stirred vigorously for 2 h. Each of these microemulsion solutions was then mixed in a reaction vessel and stirred for 8 h. In the microemulsion solution, oxidation of Mn^{2+} and reduction of Mn^{7+} occurred in the aqueous phase to form Mn^{4+}. The resulting Mn^{4+} interacted with water to produce MnO_2 [25,26]:

$$3Mn^{2+} + 2Mn^{7+} \rightarrow 5Mn^{4+} \quad (1)$$

$$Mn^{4+} + 2H_2O \rightarrow MnO_2 + 4H^+ \quad (2)$$

Since the reaction takes place only inside fixed-size aqueous droplets [27], MnO_2 particles of uniform size and shape are obtained. The MnO_2/C composite was filtered, washed with excess isopropyl alcohol to remove AOT and then dried overnight in air at 80 °C.

2.2. Preparation of MnO_2/C electrode

The MnO_2/C composite was crushed to a fine powder and then mixed with 5 wt.% Nafion in isopropyl alcohol as the binder. This mixture, in the form of a suspension called ink, was ultrasonically mixed for 30 min and then sprayed on to polished graphite plates using a spray gun. After spraying, the composite film was dried at 80 °C in air and then weighed to estimate the loading of the composite material. No annealing treatment was given to the composite powder except for X-ray diffraction analysis.

2.3. Physical and electrochemical characterization

High-resolution transmission electron microscopy (HR-TEM, JEM-30100 model) and X-ray diffraction analysis (XRD, Rigaku 405S5 with Cu Kα as the radiation source) was carried out to study the morphology, particle size and phase structure of MnO_2. An ICP-AES (inductively coupled plasma-atomic emission spectrometer; Perkin-Elmer 4300DV) was used to estimate the MnO_2 content in the MnO_2/C composite. Electrochemical characterization was carried out using a conventional three-electrode system with a platinum plate and saturated calomel (SCE) as the counter and reference electrode, respectively. Cyclic voltammograms (CV) were recorded by polarizing the working electrode between −0.1 and 0.8 V versus SCE in a 0.5 M Na_2SO_4 aqueous solution.

3. Results and discussion

The XRD patterns of the prepared MnO_2/C composite with and without annealing for 1 h are given in Fig. 1. Based on ICP analysis, the MnO_2 content of the composite was found to be 36 wt.%. The X-ray diffraction pattern for the MnO_2/C composite powder dried at 80 °C did not show any clear peaks, signifying that the manganese oxide had a highly amorphous nature. As shown in Fig. 1, however, after annealing at 200 °C, the MnO_2/C composite powder exhibits α-MnO_2 as the prominent phase with a Mn_3O_4 secondary phase. It can thus be inferred that the as-grown manganese oxide is present as an α-MnO_2 polymorph. The presence of the secondary phases can be attributed to the annealing effect, since it is known that α-MnO_2 converts to Mn_2O_3 and Mn_3O_4 at elevated temperatures [25].

The HR-TEM micrograph of the MnO_2/C composite, given in Fig. 2(a), shows a nanorod shape with 2 nm × 10 nm in size. An HR-TEM micrograph of carbon black (Vulcan XC-72),

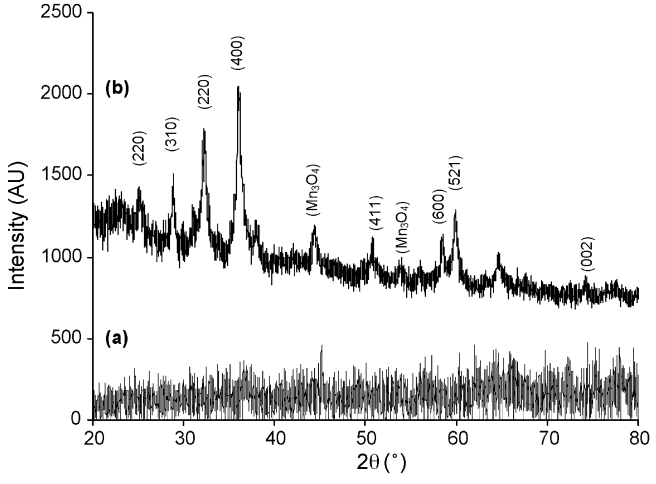

Fig. 1. X-ray diffraction patterns of MnO_2/C composite powder without binders: (a) as-grown and (b) annealed at 200 °C for 1 h.

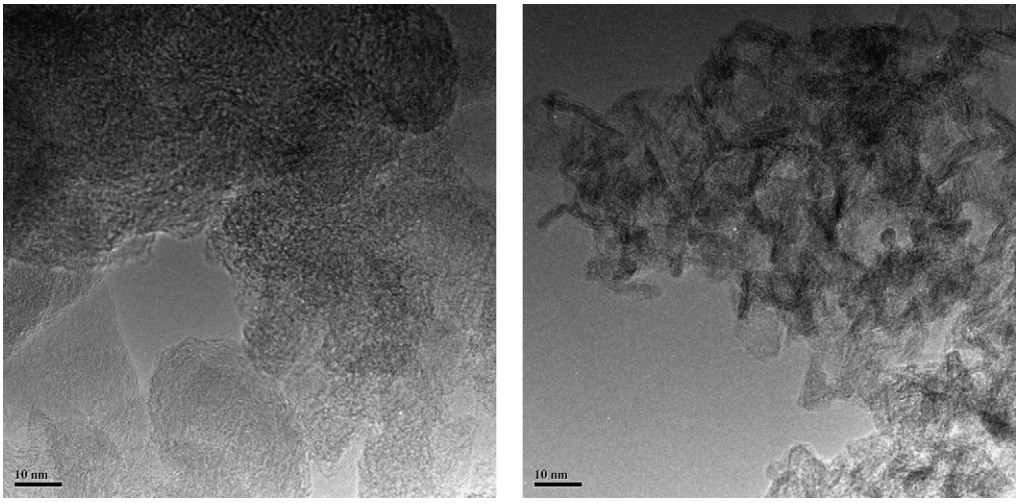

Fig. 2. HR-TEM micrographs of (a) Vulcan XC-72 carbon (left) and (b) MnO_2/C composite with 36 wt.% MnO_2 (right).

Fig. 2(b), is also presented for comparison. Interestingly, the MnO_2 nanorods are distinct and dispersed uniformly over the carbon surface with clear inter-particle boundaries. The MnO_2 nanorods produced in the present study are smaller than the MnO_2 nanorods obtained by hydrothermal (50 nm × 2.5 μm) [28] or microemulsion (40–70 nm) [25] techniques. The present study used a modified MnO_2 microemulsion synthesis process. The carbon utilized in this process is thought to provide a surface for the adsorption of nano-colloids and to thus prevent further growth of MnO_2 by agglomeration. The mechanism of MnO_2 formation in a rod-type structure is not clearly understood. It is thought that MnO_2, the reaction product of Mn(II) and Mn(VII), tends to agglomerate primarily due to the concentration and the surface energies. This rod type of 1D growth is preferred by the colloids under specific reaction conditions such as the presence of surfactant, the size of the aqueous (reactor) droplet and the MnO_2 concentration [28].

The composite electrode material (MnO_2/C) was tested by cyclic voltammetry in a 0.5 M Na_2SO_4 solution as the electrolyte. The weight ratio of electrode constituents, MnO_2:C:Nafion, was 36:59:5. For comparison, a carbon black electrode with 5 wt.% binder was also studied. Fig. 3 shows cyclic voltammograms recorded between −0.10 and 0.80 V versus SCE with and without adding MnO_2 to the carbon support with Nafion as the binder. As seen in the voltammograms, the carbon acting as the support material for the MnO_2 nanorods does not contribute much to the capacitance of composite electrode. The specific capacitance of carbon black (Vulcan XC-72) has been reported to be 27 F g^{-1} in a 1 M H_2SO_4 solution [4] and 12.6 F g^{-1} in an organic solution of 1.0 M $(C_2H_5)_4NBF_4$ in acetonitrile [29]. In the present investigation, it was found that the capacitance of carbon with 5 wt.% Nafion is about 6 F g^{-1} with 0.5 M Na_2SO_4 as the electrolyte. On the other hand, the MnO_2/C composite electrode has a reasonably high specific capacitance of 165 F g^{-1}. After subtracting the contribution of the carbon host, a high pseudocapacitance of about 458 F g^{-1} for the MnO_2 nanorods was calculated. Carbon black does not contribute significantly to the total capacitance of the electrode. Nevertheless, its presence helps MnO_2 nanorods to disperse over a large area, thereby increasing the active surface area of MnO_2. Furthermore, carbon black provides a low resistance path within the electrode, and the pores of carbon black serve as reservoirs of electrolyte that increase the ionic conductivity. In the MnO_2/C composite electrode, a major part of the specific capacitance originates as pseudocapacitance from the Mn^{4+}/Mn^{3+} reversible redox process. This process is accompanied by the reversible insertion and de-insertion of an alkali cation (Na^+) or proton (H^+) present in the electrolyte [2,26,30]. It is generally noted that, at low scan rates, the electrode material exhibits a rectangular CV shape, whereas at increasing scan rates, the shape deforms due to slow diffusion of electrolyte ions within the matrix of the electrode material [31]. An increase in the scan rate has a direct impact on the diffusion of Na^+ into the matrix, since at higher scan rates Na^+ ions will only approach the outer surface of the electrode material. Hence the surface in the deep pores does not actively contribute to the capacitance. To evaluate the rate capability of the composite electrode, cyclic voltammo-

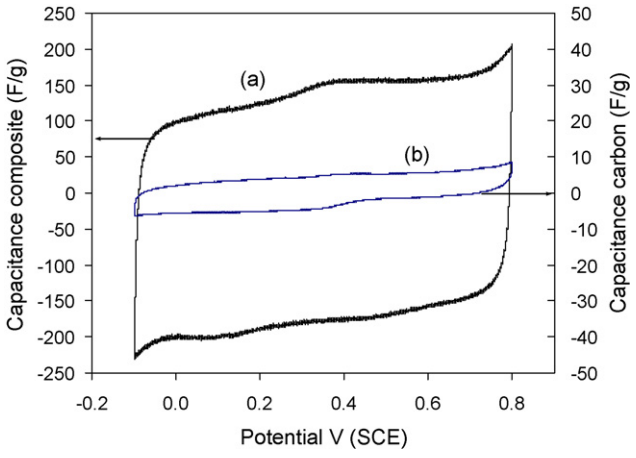

Fig. 3. Cyclic voltammograms of (a) MnO_2/C composite and (b) carbon black (with 5 wt.% Nafion) recorded between −0.1 and 0.8 V vs. SCE in 0.5 M Na_2SO_4, at a scan rate of 5 mV s^{-1}.

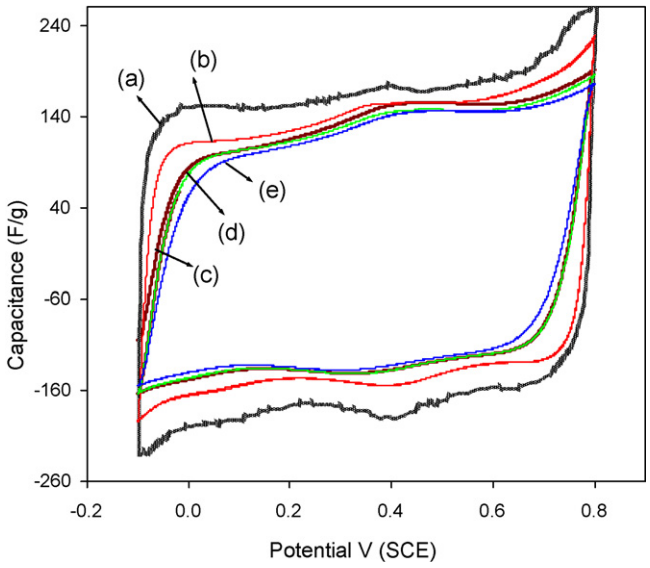

Fig. 4. Change in MnO_2/C composite electrode capacitance at increasing scan rates: (a) 5 mV s^{-1}, (b) 25 mV s^{-1}, (c) 50 mV s^{-1}, (d) 75 mV s^{-1} and (e) 100 mV s^{-1}.

grams at different scan rates were recorded and are shown in Fig. 4.

Two mechanisms are proposed for charge storage in MnO_2 electrodes. The first is based on the intercalation of H^+ or Na^+ ions in the electrode during reduction and oxidation [3,30]. The other is based on the adsorption of Na^+ ions on the electrode. Cycling the composite electrode at high rates will hinder the Na^+ ions reaching the outer surface which results in a decrease in the pseudocapacitance. As seen in Fig. 4, with increasing scan rates (5–100 mV s^{-1}), the specific capacitance of a MnO_2/C composite electrode decreases from 165 to 132 F g^{-1}. This nearly 20% decrease in total available capacity at the high cycling rate (100 mV s^{-1}) essentially shows that the carbon support provides sufficient surface area and porous channels for the transportation of electrolyte ions. Therefore, even at high scan rates, most

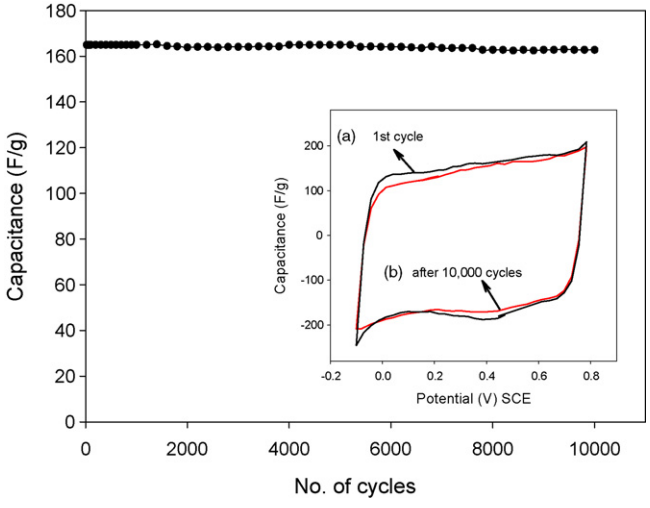

Fig. 5. Life-cycle test of MnO_2/C composite (1.2 mg cm^{-2}) electrode. Inset shows cyclic voltammograms for (a) first cycle and (b) after 10,000 cycles. The scan rate is 50 mV s^{-1}.

of the material in the composite electrode is accessible and is contributing to the redox process.

The stability and reversibility of an electrode material are important for its use in an electrochemical supercapacitor. The composite electrode (36 wt.% MnO_2) was subjected to 10,000 CV cycles in the voltage range of −0.1 to 0.8 V at 50 mV s^{-1}. The variation of electrode capacitance as a function of CV cycles is shown in Fig. 5. There is only a 3% decay in the available capacity over 10,000 cycles. This implies an excellent long-term recycling capability. Furthermore, as shown in the inset of Fig. 5, the shape of the voltammograms after 10,000 cycles confirms the highly reversible nature of the electrode material.

4. Conclusions

A microemulsion growth process to create nano-structured MnO_2/C composites for use as a highly capacitive and reversible electrode material is reported. Distinct nanorods of MnO_2, with controlled particle dimensions (2 nm × 10 nm) and uniform dispersion, have been obtained on carbon with a large surface area. An important finding is that the addition of carbon black during growth yields smaller and uniformly dispersed MnO_2 nanorods. The MnO_2/C composite exhibits a high capacitance and a long cycle-life with perfect reversibility. The specific capacitance of the MnO_2/C composite electrode in 0.5 M Na_2SO_4 is 165 F g^{-1} and that of MnO_2 is 458 F g^{-1}. Based on cycle-life tests, the MnO_2/C composite electrode has a highly stable performance up to 10,000 cycles. The long-term stability of the MnO_2/C composite electrode supports its use in supercapacitor devices.

References

[1] B.E. Conway, Electrochemical Capacitors: Scientific Fundamentals and Technological Applications, Kluwer Academic/Plenum Press, New York, 1999.
[2] M. Toupin, T. Brousse, D. Belanger, Chem. Mater. 16 (2004) 3184–3190.
[3] M. Toupin, T. Brousse, D. Belanger, Chem. Mater. 14 (2002) 3946–3952.
[4] H. Kim, B.N. Popov, J. Power Sources 104 (2002) 52–61.
[5] J.P. Zheng, P.J. Cyjan, T.R. Jow, J. Electrochem. Soc. 142 (1995) 2699–2703.
[6] C.C. Hu, T.W. Tsou, J. Power Sources 115 (2003) 179–186.
[7] H. Kim, B.N. Popov, J. Electrochem. Soc. 150 (2003) D56–D62.
[8] E.R. Pinero, V.E. Khomenko, F.E. Beguin, J. Electrochem. Soc. 152 (2005) A229–A235.
[9] K.R. Prasad, N. Miura, J. Power Sources 135 (2004) 354–360.
[10] K.R. Prasad, N. Miura, Electrochem. Commun. 6 (2004) 1004–1008.
[11] S.L. Kuo, N.L. Wu, J. Power Sources 162 (2006) 1437–1443.
[12] X. Liu, S. Fu, C. Huang, Powder Technol. 154 (2005) 120–124.
[13] Y. Xiong, Y. Xie, Z. Li, C. Wu, Chem. Eur. J. 9 (2003) 1645–1651.
[14] F. Cheng, J. Chen, X. Gou, P. Shen, Adv. Mater. 17 (2005) 2753–2756.
[15] F.A. Al-Sagheer, M.I. Zaki, Colloids Surf. A 173 (2000) 193–204.
[16] S. Devaraj, N. Munichandraiah, Electrochem. Solid State Lett. 8 (2005) A373–A377.
[17] V. Subramanian, H. Zhu, R. Vajtai, P.M. Ajayan, B. Wei, J. Phys. Chem. B 109 (2005) 20207–20214.
[18] X. Wang, Y.D. Li, Chem. Commun. 124 (2002) 764–765.
[19] M. Wei, Y. Konishi, H. Zhou, H. Sugihara, H. Arakawa, Nanotechnology 16 (2005) 245–249.
[20] D. Zheng, S. Sun, W. Fan, H. Yu, C. Fan, G. Cao, Z. Yin, X. Song, J. Phys. Chem. B 109 (2005) 16439–16443.
[21] X. Dong, W. Shen, J. Gu, L. Xiong, Y. Zhu, Hua Li, J. Shi, J. Phys. Chem. B 110 (2006) 6015–6019.

[22] V. Subramanian, H. Zhu, B. Wei, Electrochem. Commun. 8 (2006) 827–832.
[23] J.K. Chang, C.T. Lin, W.T. Tsai, Electrochem. Commun. 6 (2004) 666–671.
[24] S. Bach, M. Henry, N. Baffer, J. Livage, J. Solid State Chem. 88 (1990) 325–333.
[25] S. Devavraj, N. Munichandraiah, J. Electrochem. Soc. 154 (2007) A80–A88.
[26] H.Y. Lee, J.B. Goodenough, J. Solid State Chem. 144 (1999) 220–223.
[27] B.L. Cushing, V.L. Kolesnichenko, C.J. O'Connor, Chem. Rev. (Washington, DC) 104 (2004) 3893–3946.
[28] H. Wang, D. Qian, Z. Lu, Y. Li, R. Cheng, W. Zhang, J. Crystal Growth, in press.
[29] O. Barbieri, M. Hahn, A. Herzog, R. Kotz, Carbon 43 (2005) 1303–1310.
[30] S.C. Pang, M.A. Anderson, T.W. Chapman, J. Electrochem. Soc. 147 (2000) 444–450.
[31] S. Sarangapani, B.V. Tilak, C.P. Chen, J. Electrochem. Soc. 143 (1996) 3791–3799.